INTEGRATED STEREOLOGICAL AND BIOCHEMICAL STUDIES ON HEPATOCYTIC MEMBRANES

III. Relative Surface of Endoplasmic Reticulum Membranes in Microsomal Fractions Estimated on Freeze-Fracture Preparations

GABRIEL A. LOSA, EWALD R. WEIBEL, and ROBERT P. BOLENDER

From the Department of Anatomy, University of Berne, Berne, Switzerland. Dr. Losa's present address is the Institute for Clinical and Experimental Cancer Research, University of Berne, Tiefenau Hospital, 3004 Berne, Switzerland

ABSTRACT

New methods are required for identifying membranes in subcellular fractions with respect to their origin, if such preparations are to be evaluated morphometrically. One method is freeze-fracturing which reveals intramembrane particles whose size, pattern, and numerical density differ for various membrane types. The question is examined whether the differences in numerical particle density per square micrometer of membrane (α) can be used to differentiate membrane vesicles found in microsomal fractions from liver cells with respect to their origin in the hepatocytes. It is found that the range of α for the protoplasmic face (PF) of endoplasmic reticulum (ER) membrane $\{1{,}900 < \alpha < 3{,}250\}$ is intermediate between those for plasma and mitochondrial membranes. Since PF(ER) should appear in the outer leaflet of microsomal vesicles, α was estimated on concave profiles of freeze-fracture preparations; the numerical frequency distribution of vesicles with respect to α was trimodal, with a major peak around 2,900/μm^2 and 66% of the vesicles in the range determined for PF(ER). Using a new stereological method, it was calculated that 63% of the membrane surface in these microsomal fractions was of ER origin by this criterion. On the same preparations, an attempt was made to label the ER-derived membranes cytochemically for glucose-6-phosphatase. A line intersection count revealed 62% of the membrane surface to be of ER origin on the basis of marker enzyme labeling. These findings indicate a smaller part of ER membranes in microsomal fractions than would be predicted from biochemical data (77%). The possible reasons for such discrepancies are discussed; shifts in particle densities due to the preparation procedure could lead

to an underestimate by freeze-fracturing, whereas the prediction from biochemical data could be overestimates if marker enzymes were not homogeneously distributed.

KEY WORDS endoplasmic reticulum · freeze-etching · intramembrane particle density · membrane surface · microsomal fraction · stereology

In recent attempts to obtain a correlation between morphometric information on the membrane system of hepatocytes and biochemical data obtained on subcellular fractions (7), considerable difficulties were encountered in determining the relative area of different membrane classes in the fractions, because it was not possible to unambiguously identify the origin of a large number of smooth membrane vesicles. Various ways to overcome this difficulty can be envisaged, such as the stereological analysis combined with cytochemical labeling of membranes by their marker enzymes or with immunocytochemistry (18). In the present study, we shall primarily examine the question whether the density of intramembrane particles displayed on freeze-fracture replicas of microsomal fractions can be exploited for membrane identification in the framework of a morphometric study, but shall combine it with a stereological evaluation of cytochemically labeled fractions.

It has been shown repeatedly that the size, density, and distribution patterns of intramembrane particles displayed on freeze-fracture surfaces are characteristic for certain membrane types (8, 10, 12, 16, 17, 26, 27, 29, 30). A systematic study of freeze-fracture preparations of intact liver tissue showed that the various membrane classes of hepatocytes displayed characteristic patterns of size and density distributions of the particles in both the PF (or A) and the EF (or B).[1] Assuming that the homogenization and fractionation procedures do not alter the particle densities, we explored the possibilities of quantitatively estimating the number of microsomal vesicles derived from the various membrane classes by classifying them by particle density. This should then allow an estimation of the membrane surface area contributed to the microsomal fraction by the various organelles by a recently developed stereological method (32).

Strategy of the Proposed Analysis

In the standard fractionation procedure adopted for our studies (see reference 7 for details), the membranes of the microsomal fraction occur in the form of spherical vesicles of varying size. Upon freeze-fracturing, both concave and convex caps are displayed on the replica; the concave profiles displaying the outer, the convex caps the inner leaflet of the vesicle membrane (Fig. 1). Using a fixed angle of 45° for shadow-casting,[2] some of the caps display a shadow cast by the profile edge, to be called "cast shadow", which partly obscures membrane particles. The strategy adopted was to determine the particle density α (number of particles per square micrometer) on all *concave vesicle caps without cast shadow* and to derive from this the numerical frequency, $N_{V\alpha}$, of caps characterized by a certain particle density α. On the basis of a stereological model (32) and the known range $\{\alpha\}$[3] characterizing a certain class of membranes (e.g., endoplasmic reticulum [ER]), it should be possible to calculate the relative surface, S_S, of these membranes in the fraction.

The validity of this strategy evidently depends on whether the following basic postulates are satisfactorily fulfilled: (*a*) The various membrane classes (endoplasmic reticulum, plasma membrane, mitochondrial membranes, etc.) are unambiguously identifiable by a range of particle

[1] We are adopting the attractive new notation recently proposed by Branton et al. (9), where P stands for that leaflet of the membrane which abuts on protoplasm, and E for that abutting on external, exoplasmic, or endoplasmic spaces. In mitochondria, intermembrane space is considered to be equivalent to E, and matrix to P. The second symbol F stands for fracture face, S for surface. With respect to conventional notation, we find the following equivalences: A = PF, B = EF.

[2] The angle of 45° refers to an ideal plane formed by the knife; the true fracture "plane" being nonflat, the incidence angle of the beam may vary regionally. This is disregarded in this analysis, assuming that the angular deviations occur statistically in all directions and that their effect may therefore cancel.

[3] For convenience, we shall use the symbol α to mean both a particular particle density and the range of densities characterizing a given membrane class. Where confusion may arise, we shall use $\{. . < \alpha < . .\}$ or simply $\{\alpha\}$ to designate the range of densities.

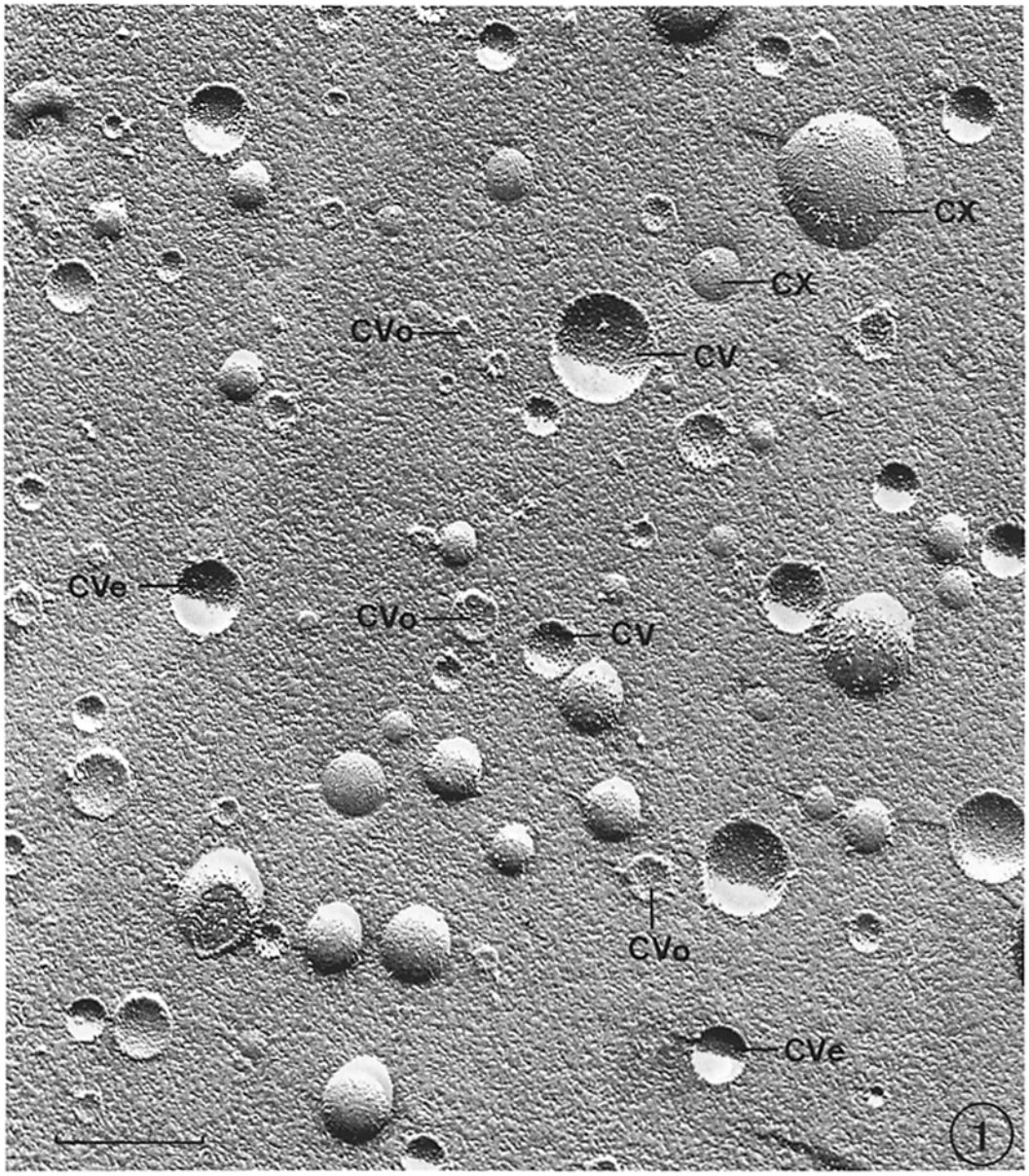

FIGURE 1 Overview of freeze-fracture replica of a microsomal fraction. Vesicles of various origin form convex (*CX*) or concave (*CV*) caps. Concave caps without cast shadow (*CVo*) are used for analysis. Note "equatorial" profiles (*CVe*) with half the cavity covered by cast shadow. Bar, 0.5 μm. × 40,000.

density $\{\alpha\}$ on concave vesicle caps; (*b*) The membranes vesiculate consistently upon homogenization; e.g., the outer leaflet of an ER cisterna consistently becomes the outer leaflet of a microsomal vesicle, etc.; (*c*) The freeze-fracture procedure and the selection of cast-shadow-free concave caps yield an unbiased sample of the vesicle population; and (*d*) A stereological method exists by which the relative surface of membranes with a certain range of particle densities can be derived from the numerical frequency of vesicles showing this particle density. It will be shown below that these postulates are satisfactorily fulfilled so that the validity of the procedure can be accepted.

Stereological Model and Method

The theoretical considerations at the basis of this model have been presented in extensive form elsewhere (32). The following is a summary of the essential points.

MODEL AND SAMPLING CONDITIONS: The microsomal fraction is considered to be composed of spherical vesicles of varying size randomly suspended in the ice matrix of the freeze-fractured specimen. If a horizontal fracture plane through the ice matrix hits the vesicles above the equator, the fracture surface is deflected upwards by the membrane, forming a convex profile; if the vesicle is hit below the equator, a concave cap is formed. The probability that a concave cap is formed is proportional to the vesicle radius.

The fracture surface is replicated by shadow-casting with platinum at an angle of 45° to the normal to the fracture plane. As a consequence, those concave caps generated by a fracture plane hitting the vesicle below the 45° tangent point will be free of cast shadow. It is found theoretically and confirmed experimentally that about 15% of the caps are concave without cast shadow irrespective of vesicle size, and that these caps constitute an unbiased sample of the vesicle population.

The particle density α is estimated by applying a test circle of fixed radius g to the center of concave caps free of cast shadow (Fig. 2). This may introduce bias for two reasons: (*a*) The area of the test circle is smaller than the surface of the cap depending on the cap's curvature, so that α may be overestimated; however, it was shown that this error is very small and can be disregarded (32); and (*b*) Caps smaller than the test circle are lost, and this will affect the small vesicle population more seriously than the larger vesicles; this second error may be appreciable and has to be corrected for.

It was shown by theoretical considerations (32) that the required correction factor depends on the size distribution of the $\{\alpha\}$ vesicle population in relation to the size distribution of the total vesicle population. Designating by E_α (.) and E_T (.) the expected (mean) values of the size parameter (.)

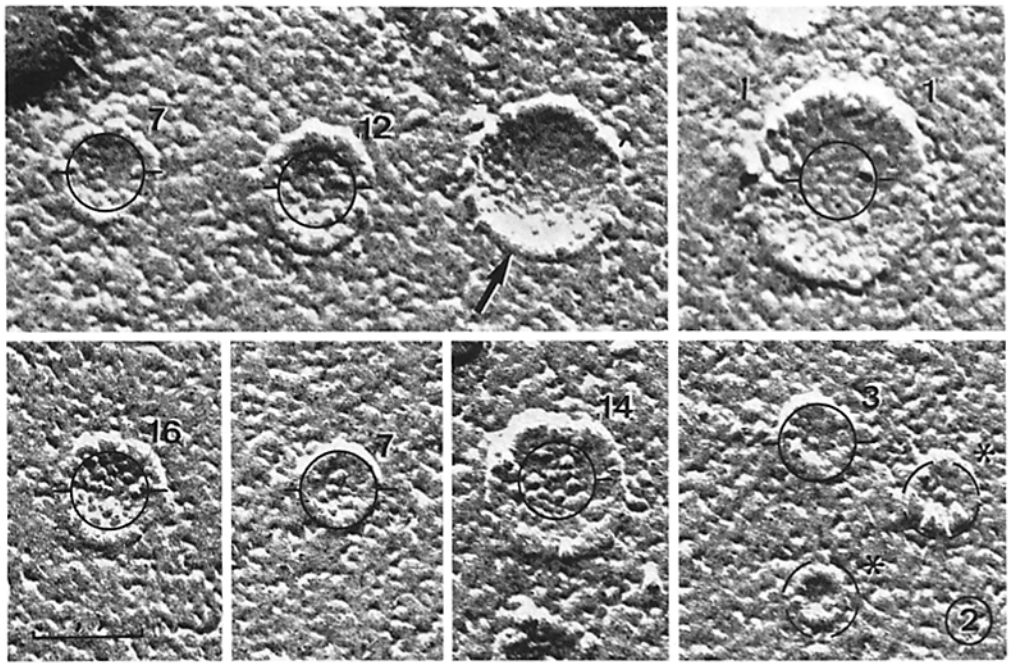

FIGURE 2 Montage of concave vesicle profiles at actual magnification used for particle counting. Test circles are superimposed and the particle numbers counted indicated. Arrow indicates profile not evaluated because of cast shadow. Asterisks mark profiles lost because they are smaller than the test circle. Bar, 0.1 μm. × 145,000.

in the $\{\alpha\}$ vesicle population and the total (T) population. Designating by E_α (.) and E_T (.) the expected (mean) values of the size parameter (.) from the observed relative number of vesicles with particle density $\{\alpha\}$ ($N_{N\alpha}$) by

$$S_{S\alpha} = N_{N\alpha} \times \frac{E_\alpha(q^2)/\{E_\alpha(\sqrt{q^2-1}) - \sqrt{\tfrac{1}{2}}E_\alpha(q)\}}{E_T(q^2)/\{E_T(\sqrt{q^2-1}) - \sqrt{\tfrac{1}{2}}E_T(q)\}}$$

$$= N_{N\alpha} \times \left\{\frac{\lambda_\alpha}{\lambda_T}\right\}, \quad (1)$$

where $q = r/g$ is the vesicle radius measured in units of test circle radius g.

The relative membrane area of α vesicles can hence be derived from the estimated numerical frequency $N_{N\alpha}$ if the size-distribution-dependent coefficient

$$\lambda = \frac{E(q^2)}{\{E(\sqrt{q^2-1}) - \sqrt{\tfrac{1}{2}}E(q)\}}, \quad (2)$$

can be estimated for the total vesicle population and for $\{\alpha\}$ vesicles.

MATERIALS AND METHODS

Specimen Preparation

Male Sprague-Dawley rats (160–200-g body weight) were fasted for 18 h before sacrifice by decapitation. After rapid removal of the liver, small tissue blocks were fixed for 15 min with 1.5% glutaraldehyde in 0.1 M Na cacodylate buffer (pH 7.4, ice-cold). Before being fractured, the tissue blocks were treated for 15 min with 30% glycerol in cacodylate buffer (0.1 M, pH 7.4, ice-cold). The remaining liver tissue was placed into an ice-cold 0.25 M sucrose solution at pH 7.4 containing 3 mM imidazole, weighed, and carefully homogenized with a Potter homogenizer (3431-E55; Arthur H. Thomas Co., Philadelphia, Pa.) at 700 rpm, one stroke down and up.

Differential centrifugation was performed in a Beckman L-2/65 B centrifuge (Beckman Instruments, Inc., Spinco Div., Palo Alto, Calif.) with a rotor type 40, according to De Duve et al. (11); details of the procedure are given in reference 7. Microsomal membranes were pelleted from the post ML (ML = large granule fraction) supernate at 6 million g-min. A 1-ml aliquot of the microsomal suspension (diluted 1:5 with 0.25 M buffered sucrose) was added to 10 ml of a 30% glycerol-water solution, thoroughly mixed, and re-pelleted at 39,000 rpm for 30 min. The supernate was discarded and the microsomal pellet gently homogenized with a Dounce pestle (Kontes Co., Vineland, N. J.) in the centrifuge tube to obtain a uniform suspension. Tissue blocks and drops of the microsomal samples were placed on supporting gold disks, quick-frozen in Freon 22 at −150°C, and stored in liquid nitrogen (−196°C) until fracturing.

The samples were fractured and etched (1 min) at −100°C and 2×10^{-6} torr in a Balzers freeze-etching apparatus (BA 360 M; Balzers AG, Balzers, Liechtenstein). Replicas were obtained by shadowing the fracture surface with platinum and carbon at a fixed angle of 45° followed with carbon at 90°, using an electron gun evaporator and an oscillating quartz for monitoring thickness of the replica (24, 25). The replicas were cleaned with household bleach (1–4 h) followed by 70% sulfuric acid (12–36 h).

Stereological Procedure for Particle Density Estimation

The replicas were examined at 80 kV with a Philips 300 electron microscope, and pictures were taken on 35-mm film. To determine the exact magnification, a micrograph of a calibration grating (Ernest F. Fullam, Inc., Schenectady, N. Y.) was recorded on each film strip (31). Positive film prints of these negatives were evaluated in a projection device (31) which enlarged the micrographs 10 times to a final magnification of 130,000–143,000. Particle densities per unit area of membrane fracture-face were determined by applying a test circle of 9-mm diameter (area $A = 3.4 \times 10^{-3}$ μm^2) to the fracture-faces (Fig. 2). All particles that were totally enclosed and those intersecting the upper hemicircle were counted, those intersecting the lower hemicircle were rejected. This test circle size, which enclosed up to 17 particles, was chosen to afford easy counting and satisfactory resolution of particle density. Since the test circle appeared to eliminate a relatively large fraction of the small vesicles, a second evaluation was performed in one case using a circle of 6-mm diameter ($A = 1.68 \times 10^{-3}$ μm^2); as will be shown below (Table II), this did not affect the results in an appreciable manner. The larger test circle was therefore retained for the main part of the study.

In microsomal fraction preparations, the test circle was centered to the vesicle profile with the hemicircle marks kept horizontal (Fig. 2); only concave profiles free of cast shadow were used. In intact cell preparations, a set of test circles was randomly placed onto "horizontal" fracture planes of the various membrane types. For each microsomal preparation, 150–300 test-circle applications were used. The intact tissue standards were determined with ~60–100 circle applications per membrane type.

Estimation of Relative ER Membrane by Cytochemical Labeling

An aliquot of the microsomal fractions was collected by filtration onto Millipore filters (pore size 0.025 μm;

Millipore Corp., Bedford, Mass.) according to Baudhuin et al. (4), after the fractions had reacted for glucose-6-phosphatase using the following procedure based on the method of Leskes et al. (20). A 0.1-ml aliquot of the microsomal suspension diluted 10 times with a 0.25-M sucrose solution was mixed with 1.5 ml of a medium containing 1 mM D-glucose-6-phosphate (Dipotassium salt, Sigma Chemical Co., St. Louis, Mo.), 2 mM $Pb(NO_3)_2$, and 0.05 M Na cacodylate buffer at pH 7.4, and incubated at room temperature for 20 min. The suspension was then mixed with 1.5 ml of 1% OsO_4 buffered with 0.1 M Na cacodylate and transferred into the filtration cylinder to produce a pellicle by filtering it at a gauge pressure of 1 atm of N_2. The pellicle was then removed, postfixed for 2 h in buffered osmium tetroxide, and processed for Epon embedding as outlined in reference 7. Cytochemical controls were performed with the same procedure, except that the reaction medium was substrate-free.

The relative membrane surface area labeled with the reaction product was determined on thin sections, by an intersection counting procedure. The pellicles were cut perpendicular to the surface and micrographs were recorded throughout the depth of the pellicle (7). A square grid of 12 × 12 test lines was applied, and intersections with membrane traces of "glucose-6-phosphatase"-positive and -negative vesicles were counted.[4] The relative surface of "positive" membranes was estimated by the ratio of "positive" intersections to all intersections. Because no great discrepancy in the size distribution between positive and negative vesicles was detected, no corrections for section thickness effects were introduced (33).

Biochemical Controls

To assess the composition of the microsomal fractions, an aliquot was assayed for the following marker enzymes, according to the methods described elsewhere: 5′-nucleotidase (15), glucose-6-phosphatase (11), monoamine oxidase (MAO) (3), acid phosphatase (2), and protein (22). Total and specific activities were calculated.

RESULTS

Particle Density Characteristics of Cytoplasmic Membranes in Intact Hepatocytes

The characterization of membranes from freeze-fracture preparations of intact tissue by means of particle density was restricted to the major membrane classes of hepatocytes, namely plasma membrane, endoplasmic reticulum, and mitochondria. Attempts were also made to include other smooth-surfaced membranes, such as Golgi apparatus and lysosomes, but they were found to be difficult to characterize reliably on freeze etching replicas, mainly because of their rarity. Fig. 3 shows examples of the various fracture-faces examined. The distributions of particle densities are shown in Fig. 4 whereas Table I summarizes the distribution parameters.

Particle densities in the plasma membrane were separately determined on areas of the lateral, sinusoidal, and canalicular portions. For all three regions of the plasma membrane, the ranges of particle density were similar on EF $\{0 < \alpha < 1{,}900\}$, but quite different on the protoplasmic leaflet (Table I). On PF of the lateral and sinusoidal portions, the particle density was in the range $\{2{,}500 < \alpha < 5{,}000\}$, whereas the canalicular membranes showed an unusually high density $\{4{,}370 < \alpha < 6{,}000\}$. The particle density standards for the endoplasmic reticulum were separately determined for rough cisternae, and for smooth tubules. The ranges of particle density observed with $\{0 < \alpha < 1{,}950\}$ for EF (peak at 730) and $\{1{,}900 < \alpha < 3{,}700\}$ for PF (peak at 2,920). It is noted that α (PF) for smooth ER (SER) is in the same range, but slightly shifted to lower values with the peak at 2,640 (Table I and Fig. 4).

Mitochondrial areas are easily identified if they show fracture-faces of both outer and inner membranes (Fig. 3): if the outer membrane displays its PF, then the patches of inner membrane attached to it show their EF and vice versa. Fig. 3 shows convex portions of the particle-rich inner membrane (PF) which underlie the smoother "inner" face EF of the outer membrane. On concave mitochondrial profiles, the inner membrane is often torn away, leaving irregularly distributed patches of EF on the underlying PF of the outer membrane. As shown in Fig. 4, the ranges of particle density $\{\alpha\}$ were similar to those for lateral plasma membrane, with some shifts in the peak densities, particularly with EF of the outer mitochondrial membrane.

The most important observations are (*a*) that the ranges of particle density for EF and PF are clearly separated in all instances, and (*b*) that PF of endoplasmic reticulum membranes has a range of particle densities $\{1{,}900 < \alpha < 3{,}700\}$ which is intermediate to those in EF and PF of the other membrane types.

[4] Any vesicle containing some reaction product was counted as "positive", i.e., as ER-derived.

Vesiculation of Membranes upon Homogenization

Since the stereological approach proposed focuses on concave vesicle profiles (thus viewing the fracture-face of the outer leaflet of the vesicle membrane), the approach is only valid if this outer leaflet represents, for each membrane class, consistently either the P or the E leaflet. This raises the question of the consistency of vesiculation of each membrane type. With respect to rough ER (RER), it has been shown repeatedly (19) that ribosomes are always on the outer surface of the RER vesicles (Fig. 5); consequently, the fracture-face of the outer vesicle leaflet corresponds to PF. The same holds probably true for SER tubules.

Many of the smooth vesicles may be derived from mitochondrial membranes, since it was shown elsewhere (7) that an important part of the mitochondrial membranes is lost from these organelles, probably as a consequence of their fragmentation. From the observation of bleb formations on isolated mitochondria, it is likely that outer membrane fragments vesiculate with the intermembrane space inwards, the observed fracture-face of the outer leaflet thus being PF. For inner membranes the situation is not clear; it appears possible that cristae, which are often swollen, vesiculate with the intracristal space inwards, whereas the peripheral inner membrane could well vesiculate by enclosing the matrix space. This needs to be clarified, but is of little consequence for the present study.

The evidence so far available indicates that the plasma membrane fragments found in the microsomal fraction have vesiculated predominantly by enclosing the protoplasmic space, so that the observed fracture-face of the outer leaflet should correspond to EF. The evidence is the following: (*a*) on thin sections of *P* fractions many vesicles containing fuzzy filamentous material attached to the membrane interior are found (Fig. 5), whereas vesicles with a fuzzy surface layer are rarely encountered; and (*b*) in a freeze-fracture study of isolated plasma membrane vesicles, the particle density found on the concave fracture-faces was $\{\alpha < 1{,}900\}$ in >85% of the vesicles and thus corresponded to $\{\alpha\}$ of EF of plasma membranes (21).

Fig. 4 shows that the distribution of particle densities can be described reasonably well by a normal distribution for all those faces which should contribute concave profiles (solid lines). The range $\{\bar{\alpha} \pm 2 \text{ SD}\}$ should hence comprise 95% of all the profiles. As calculated from Table I, these ranges are as follows:

Plasma membrane (EF)	
sinusoidal	$\{0 < \alpha < 1{,}596\}$
lateral	$\{430 < \alpha < 2{,}110\}$
canalicular	$\{57 < \alpha <, 1{,}693\}$
Mitochondrial inner membrane (EF)	$\{430 < \alpha <, 2{,}030\}$
Endoplasmic reticulum (PF)	
RER	$\{2{,}305 < \alpha < 3{,}545\}$
SER	$\{2{,}130 < \alpha < 3{,}210\}$
Mitochondrial outer membrane (PF)	$\{3{,}090 < \alpha < 5{,}050\}$

From this analysis, we conclude that profiles derived from ER should be well separated from those originating from plasma membrane and inner mitochondrial membrane. There is a certain overlap with the tail of outer mitochondrial membrane vesicles (Fig. 4), but this tail represents a few percent of the outer mitochondrial membranes. It appears hence that it should be possible to estimate the fraction of vesicles derived from ER, whereas it is impossible to clearly identify the other membrane classes, perhaps with the exception of outer mitochondrial membranes which should all be included in the profiles with particle densities $\{\alpha > 3{,}500\}$.

Estimation of Relative Number of ER Vesicles

The particle density α was determined on microsomal vesicles collected from four *P* fractions, using three replicas from each fraction. Table II shows that the distribution of the counts was very reproducible, as well between replicas as between preparations. In all four cases, the frequency distribution of α was trimodal (Fig. 6) with a major peak at $\alpha \approx 2{,}900$ and two lower peaks around $\alpha \approx 1{,}000$ and 4,200, respectively. It is evident that the major part of the profiles belongs to the vesicle population with a particle density in the range $\{2{,}100 < \alpha < 3{,}500\ \mu\text{m}^{-2}\}$, the range corresponding to endoplasmic reticulum.

Table II shows furthermore on one experiment that the choice of a smaller test circle does not influence the distribution of vesicles to the three particle-density classes.

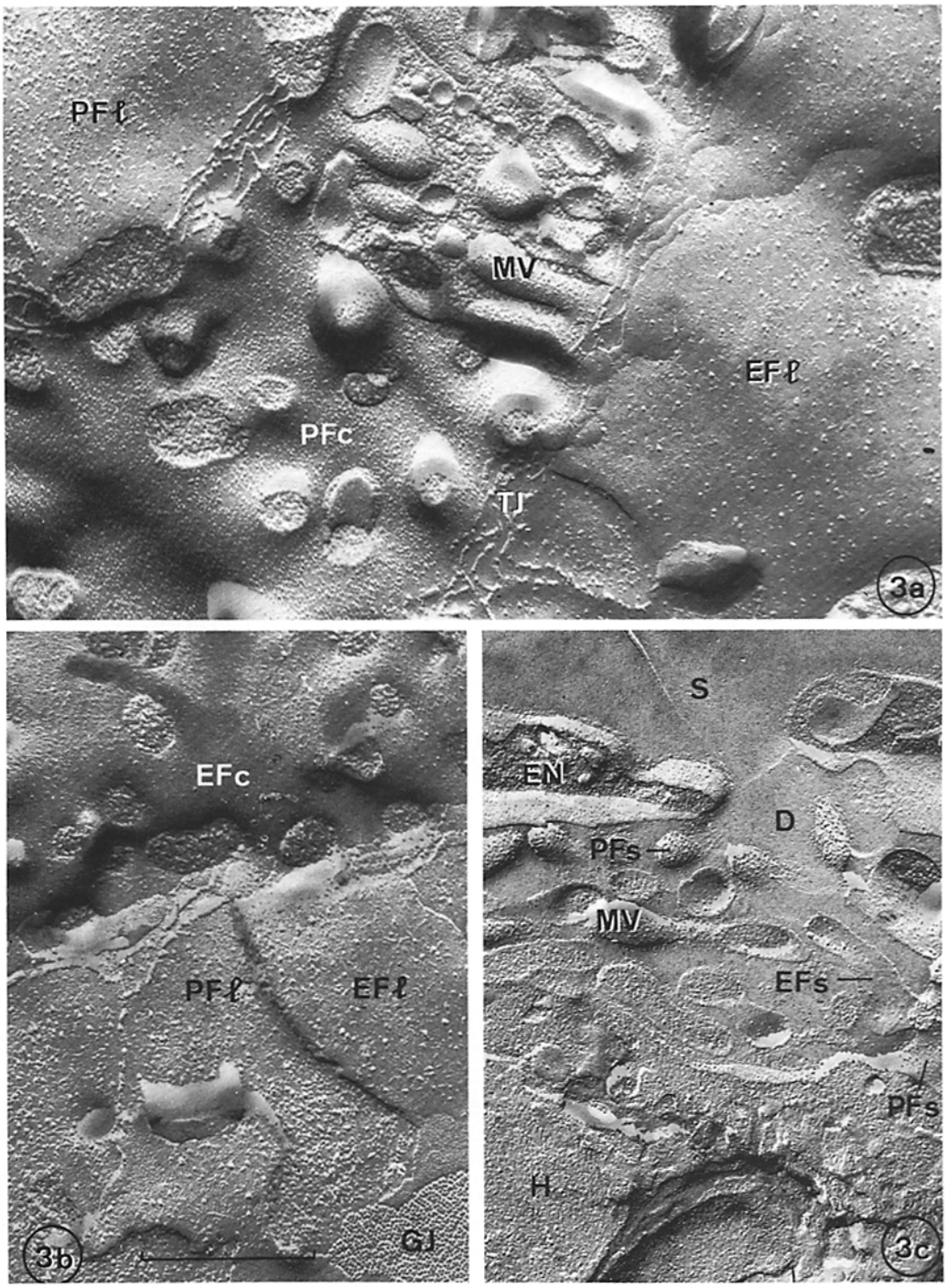

FIGURE 3 Freeze-fracture replicas of intact hepatocytes on which tissue standards for particle densities were estimated at about three times higher magnification. External and protoplasmic fracture-faces identified by *EF* and *PF*. Bar, 0.5 μm. × 50,000. (*a-c*) Lateral (*l*), canalicular (*c*), and sinusoidal (*s*) face of plasmalemma, with tight (*TJ*) and gap junctions (*GJ*) and microvilli (*MV*). Fig. 3*c* shows sinusoidal (*S*) and Disse's (*D*) spaces, endothelial cell (*EN*), and hepatocyte (*H*). (*d*) Endoplasmic reticulum in cisternal (*rer*) and tubular form (*ser*), and Golgi complex (*go*). (*e* and *f*) Profiles of mitochondria showing fracture-faces of inner (*mi*) and outer (*mo*) membranes.

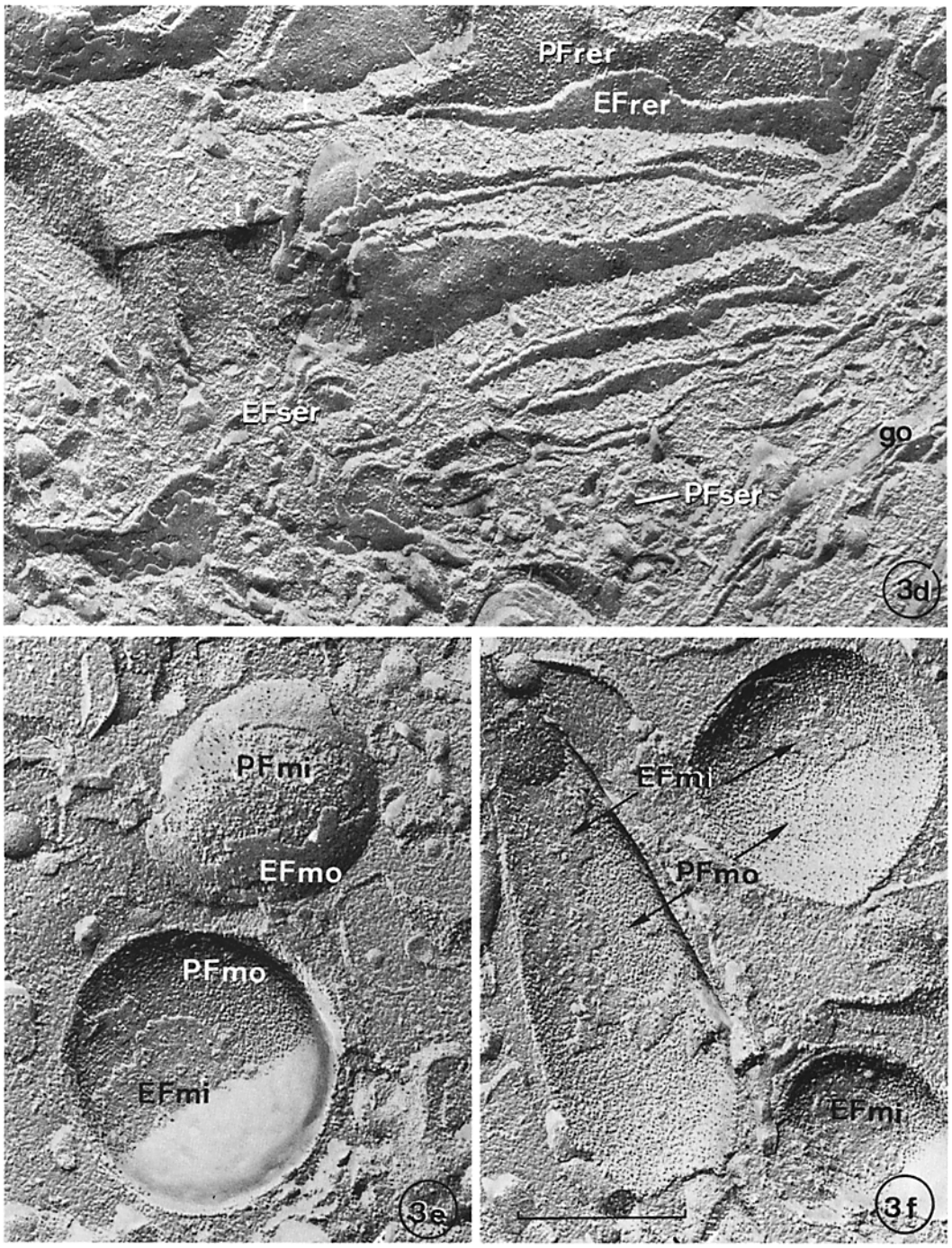

Size Distribution of Microsomal Vesicles

The calculation of relative surface area by the model described above depends on the size distribution of microsomal vesicles included in the sample. Concave caps with half their area covered by cast shadow represent equatorial cuts of the vesicles; the size distribution of such caps yields directly the actual vesicle size distribution. As

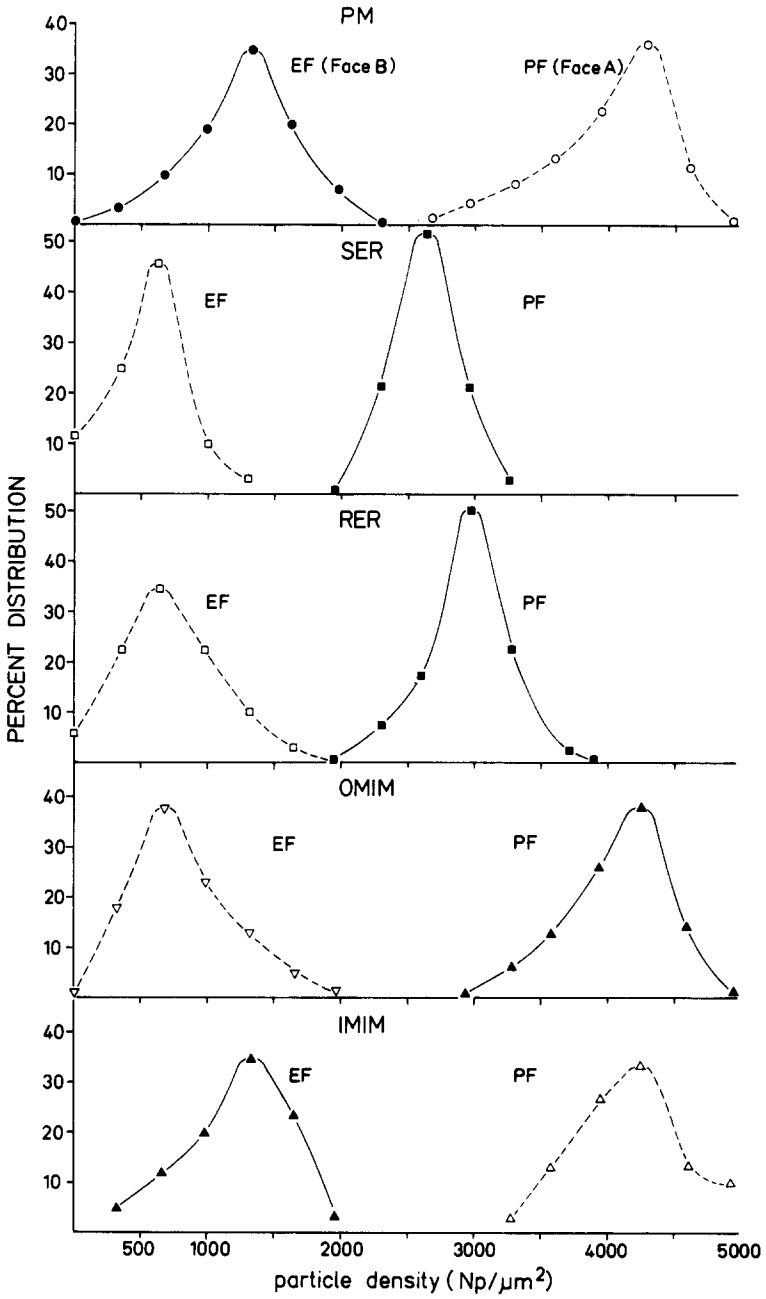

FIGURE 4 Distribution of intramembranous particle densities on membrane fracture-faces of intact hepatocytes. Fracture-faces which are thought to correspond to the outer leaflet or concave face of the vesicles present in the microsomal fraction are represented with a continuous line. *IMIM*, inner mitochondrial membrane. *OMIM*, outer mitochondria membrane.

shown in Fig. 7, this distribution is bimodal with a sharp peak at 0.13 μm, and a lower one at 0.06 μm; a flat tail extends up to 0.36 μm. The mean vesicle diameter is 0.142 μm, and the mean membrane surface is 1.58×10^{-2} μm^2.

Differentiation of vesicles is only possible on cast-shadow-free caps; Fig. 7 shows that the size distribution of such profiles is similar in shape but

TABLE I

Particle Densities on Membrane Fracture-Faces for Intact Hepatocytes

		Range	Mean	SD
Plasma membrane			~900	*g* 420
Lateral	PF	$2,600 < \alpha < 5,000$	4,020	550
	EF	$0 < \alpha < 2,300$	1,270	420
Sinusoidal	PF	$2,460 < \alpha < 4,370$	3,545	403
	EF	$0 < \alpha < 1,900$	680	458
Canalicular	PF	$4,370 < \alpha < 6,000$	5,240	346
	EF	$0 < \alpha < 1,900$	875	409
Endoplasmic reticulum				
RER	PF	$2,300 < \alpha < 3,700$	2,925	310
	EF	$0 < \alpha < 1,950$	730	403
SER	PF	$1,900 < \alpha < 3,250$	2,670	270
	EF	$0 < \alpha < 1,340$	545	315
Total ER	PF	$1,900 < \alpha < 3,700$	2,725	–
	EF	$0 < \alpha < 1,950$	640	–
Mitochondria				
Outer membrane	PF	$3,000 < \alpha < 5,000$	4,070	490
	EF	$0 < \alpha < 2,000$	820	410
Inner membrane	PF	$3,300 < \alpha < 5,000$	4,210	420
	EF	$0 < \alpha < 2,000$	1,230	400
Lysosomes	PF	$3,250 < \alpha < 4,680$	3,940	310
Golgi apparatus	PF	$0 < \alpha < 1,700$	870	300

α was determined with a test circle of area $A = 3.4 \times 10^{-3}$ μm^2, as used for the microsomal preparations; this influences the standard deviation estimate (SD).

shifted towards smaller values. From geometric considerations, one would expect the diameter of a cast-shadow-free cap to be smaller than the vesicle diameter by a factor of about $\sqrt{1/2} = 0.71$. It is evident from Fig. 7 that the peaks, the largest values observed, and the means of the two distributions are shifted by about this factor; the cap size distribution hence approximates the vesicle size distribution if the scaling factor $\sqrt{1/2}$ is considered.

In a first approximation, it is possible to estimate the size frequency distribution of vesicles derived from the various membrane classes by differentiating cast-shadow-free caps on the basis of their particle density. The result of this analysis is shown in Fig. 8. Note that the data for Fig. 8 have been obtained on a specimen other than those for Fig. 7; the good agreement between the total cap size distributions (open circles) indicates that the vesicle size distribution is similar from preparation to preparation.

It is evident that the cap size distribution of ER-derived vesicles is very similar to the overall cap size distribution, whereas that for other membranes differs to some extent. On the basis of the comparison of cap and vesicle size distributions (Figs. 7 and 8), the size distributions of caps shown in Fig. 6 can be approximately transformed to vesicle size distribution by multiplying with the scaling factor $\sqrt{2}$.

Calculation of Relative Membrane Surface of ER-Derived Vesicles

The calculation of the relative membrane surface contributed to the microsomal fraction by vesicles derived from ER, $S_S(er)$, depends on the relative number of such vesicles, $N_V(er)$, and on a size distribution-dependent correction factor, λ_{er}/λ_T, as defined in Eqs. 1 and 2.

The parameters entering λ can be approximately calculated from the cap size distributions of Fig. 8 by letting

$$q = (\sqrt{2} \cdot d)/2g, \tag{3}$$

where d is the observed cap diameter and $2g$ the

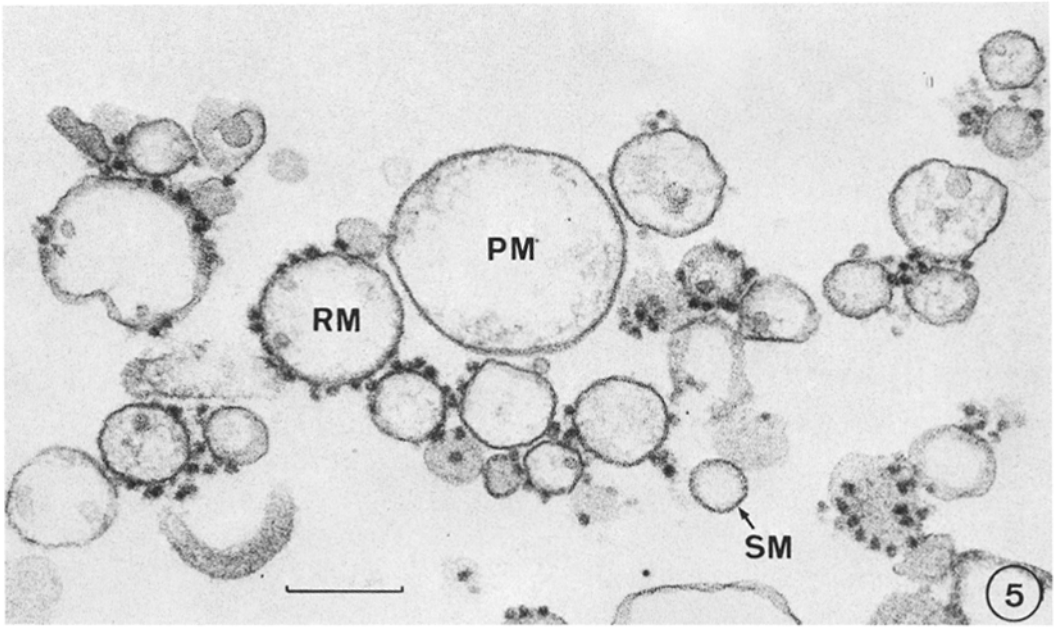

FIGURE 5 Section of pellicle obtained by filtration of microsomal suspension. RER vesicles bearing ribosomes (*RM*) are readily identified, whereas the origin of the smooth membranes (*SM*) is uncertain. Note vesicle (*PM*) presumably derived from plasma membrane with "fuzzy" content. Bar, 0.5 μm. × 62,700.

TABLE II

Numerical Frequency of Microsomal Vesicles by Particle Density Range

		Numerical frequency ($N_{\%}$) in %				
		1*	2*	3*	4*	4‡
{0 < α < 2,100}	a	16.7	17.9	16.0	17.1	17.7
	b	16.2	17.7	18.2	15.3	17.8
	c	18.6	17.7	17.8	16.7	21.2
{2,100 ≤ α < 3,500}	a	66.7	64.3	66.0	64.3	63.8
	b	66.2	63.7	68.2	64.4	61.4
	c	62.7	60.8	66.7	63.9	62.1
{3,500 ≤ α < 5,000}	a	16.7	17.9	18.0	18.6	18.5
	b	17.7	18.6	13.6	20.3	20.8
	c	18.6	21.5	15.6	19.4	18.7

* For each of the four preparations (1 - 4), three replicas (*a* - *c*) were evaluated using a test circle of area $A = 3.4 \times 10^{-3}$ μm^2.

‡ A second count was done on preparation 4 with a smaller test circle of area $A = 1.7 \times 10^{-3}$ μm^2.

test circle diameter. With $f(q)$ as the relative frequency of vesicles of diameter q the formulas are

$$E(q) = \sum f(q) \cdot q, \quad (4)$$

$$E(q^2) = \sum f(q) \cdot q^2, \quad (5)$$

$$E(\sqrt{q^2 - 1}) = \sum f(q) \cdot \sqrt{q^2 - 1}. \quad (6)$$

Table III shows the result of this calculation for

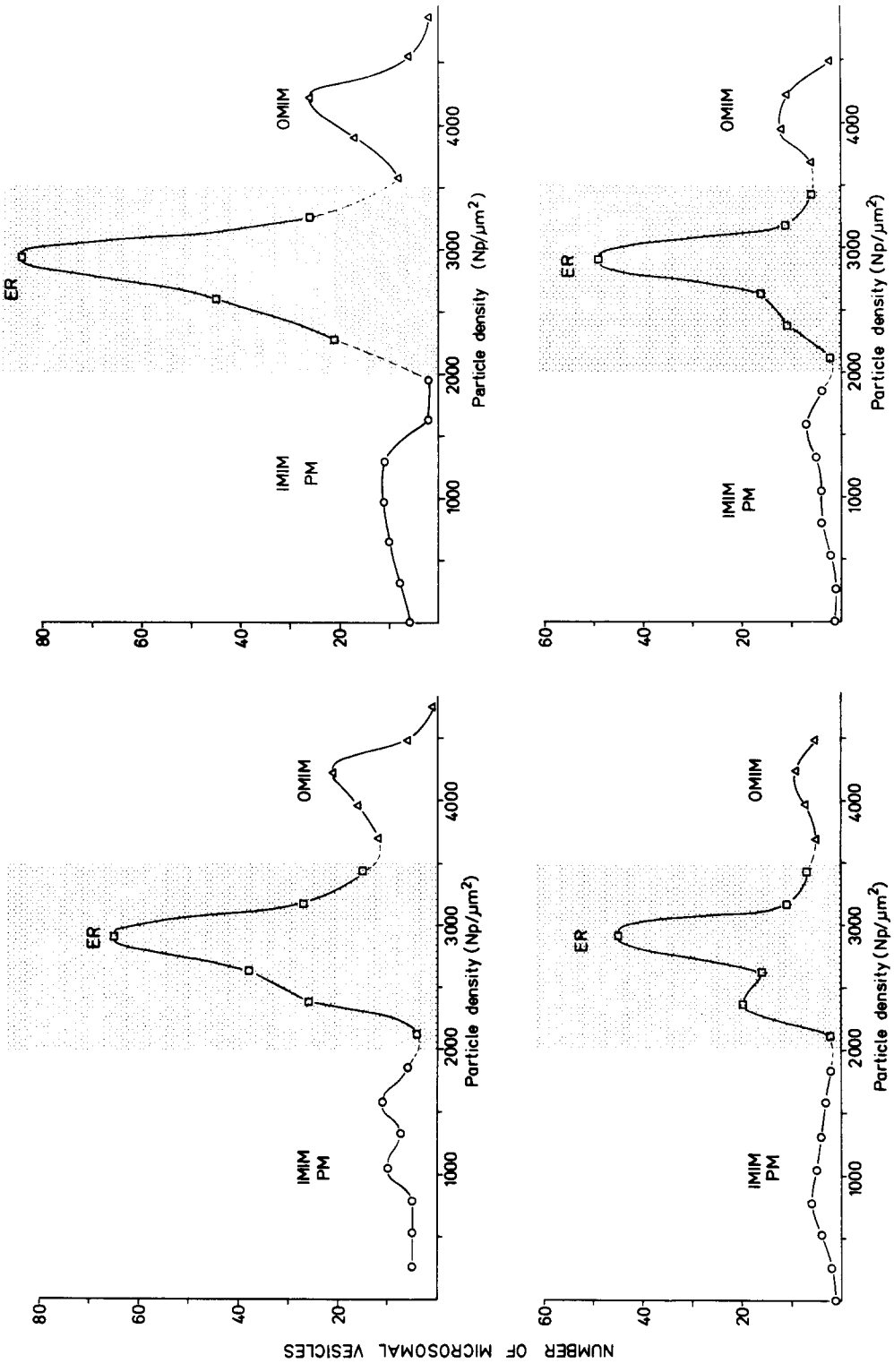

FIGURE 6 Distribution of number of microsomal vesicles without cast shadow with respect to particle density for all four microsomal preparations. Shaded area indicates range for ER-derived membranes.

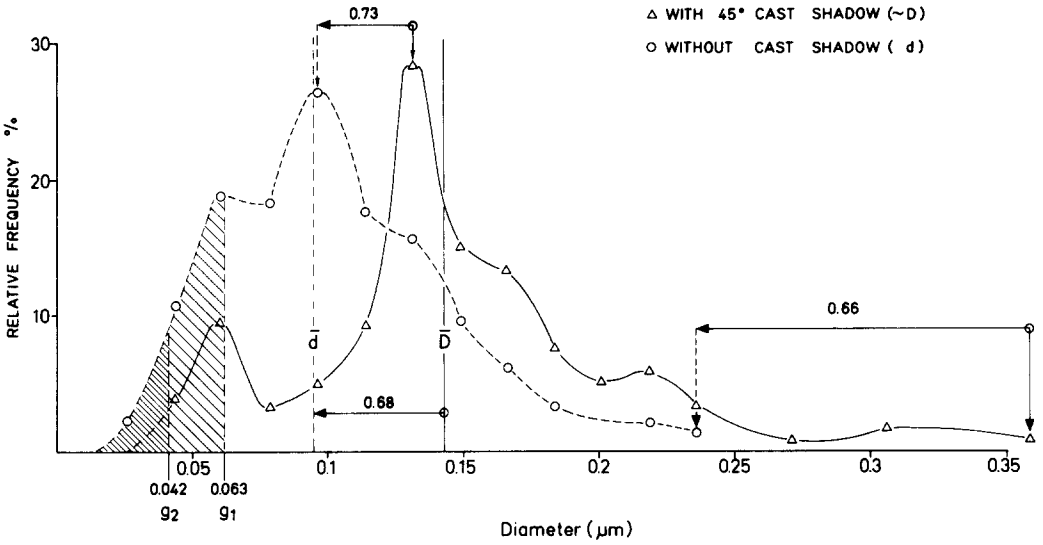

FIGURE 7 Size distribution of diameter D of microsomal vesicles measured on "equatorial profiles" (cf. Fig. 1 *CVe*), and of cap diameter d of caps without cast shadow (*CVo* in Fig. 1). The size was estimated by measuring the diameter of the vesicles perpendicular to the shadowing direction. Profiles smaller than test circle diameter g_1 or g_2 are lost (shaded area).

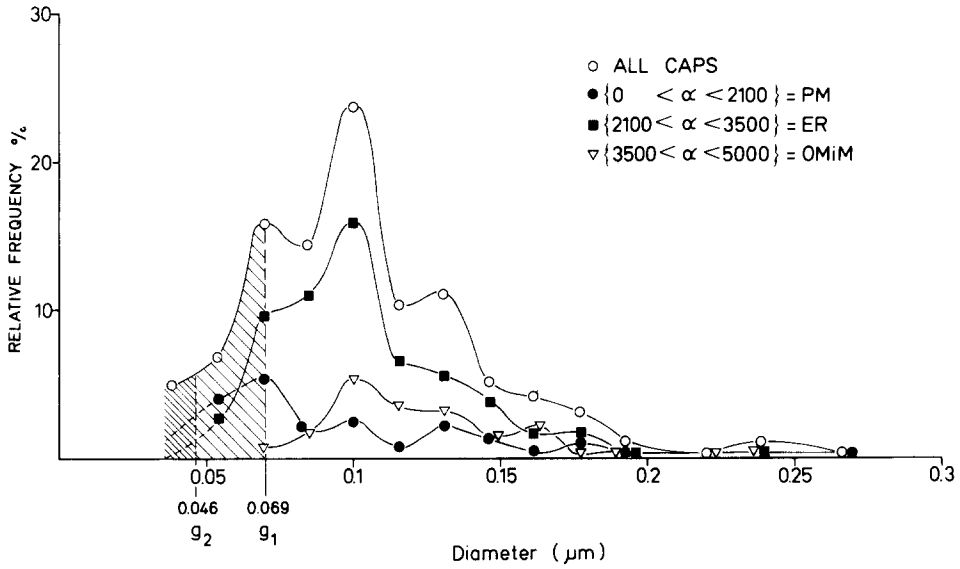

FIGURE 8 Size distribution of microsomal vesicles without cast shadow after identification by means of particle density. ER-derived vesicles have size distribution similar to that of the overall vesicle population (○). Profiles smaller than the test circle diameters g_1 or g_2 are lost (shaded area). Classification of caps by particle density was made using the smaller test circle (g_2).

the two test circle sizes employed. It is seen that the correction factor λ_{er}/λ_T differs only slightly from 1, and that the errors introduced by the two test circle sizes differ very little.

The relative number of vesicles derived from ER is given in Table II. Considering the correction factors for size distribution effects, it is found that 62.8% (SE ± 0.56%) of the microsomal mem-

TABLE III

Size Distribution Correction Factors

	$2g$ = 0.069 μm		$2g$ = 0.046 μm	
	ER	Total	ER	Total
E (q^2)	5.944	6.383	11.59	12.21
E ($\sqrt{q^2-1}$)	2.145	2.210	3.06	3.13
E (q)	2.378	2.440	3.24	3.31
λ	12.936	13.171	14.99	15.38
λ_{er}/λ_T	0.982		0.975	

branes are derived from endoplasmic reticulum (Fig. 9).

It is difficult to estimate the "true" relative surface of membranes belonging to the two other classes of particle density; the number of vesicles observed was too small to reliably estimate the size distribution factors. One finds from Fig. 8 that plasma membrane vesicles are in a smaller size range, and those derived from mitochondrial outer membrane in a higher size range; accordingly, the correction factors are >1 for plasma membrane and <1 for mitochondrial outer membrane. In Fig. 9, the estimated relative surface areas of these membrane classes are also plotted.

Comparative Estimation of Relative ER Surface Area by Glucose-6-Phosphatase Labeling

Aliquots of the same four fractions had reacted for glucose-6-phosphatase for cytochemical labeling of vesicles derived from ER. The relative membrane surface area of labeled vesicles, $S_S(g6p)$, as obtained by an intersection count on thin sections, was found to be 61.8% (SE ± 1.46%). This compares well with $S_S(er)$ estimated from the particle density evaluation (Fig. 9).

Biochemical Characterization of Fractions

Table IV reports the total activities of various marker enzymes, expressed as units per gram of liver, and determined in the following fractions: *E* (extract), *N* (nuclear), *M* (heavy mitochondrial), *L* (light mitochondrial), *P* (microsomal), and *S* (supernate). Means (± 1 SE) of all four experiments are given. Recoveries were 93–99%.

These data show that the fractions are not homogeneous with respect to membrane type but contaminated at different degrees with fragments of various cellular membranes. The microsomal

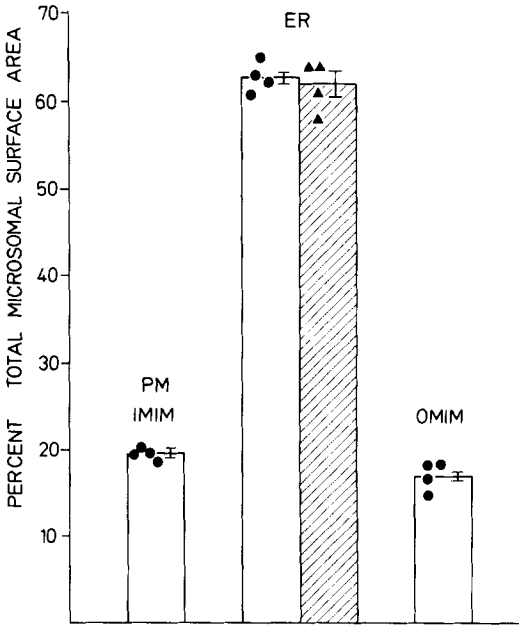

FIGURE 9 Membrane surface distribution in microsomal fraction to three membrane classes, expressed as percent of the total microsomal surface area. Open columns refer to the result of the analysis of freeze-fracture preparations (mean ± 1 SE, and data for individual preparation). Shaded column reports result of cytochemistry (glucose-6-phosphatase-positive membranes).

fraction contains ~58% of the total glucose-6-phosphatase activity, ~25% of the total 5'-nucleotidase activity, and ~14% of monoamine oxidase and acid phosphatase.

DISCUSSION

The most striking—and perhaps disturbing—observation of this study is the finding that only 63% of the microsomal membrane surface appears to be derived from endoplasmic reticulum. Although it is generally recognized that microsomal *P* fractions, as they are obtained by differential centrifugation, contain an appreciable amount of membranes derived from subcellular sites other than endoplasmic reticulum, biochemical data in general indicate a lesser degree of contamination. Beaufay et al. (5) have recently estimated that "microsomal elements deriving from ER account ... for no more than 77% of microsomal protein". The difference between 77 and 63% is evidently appreciable, particularly because the methods of preparing the *P* fractions were essen-

TABLE IV

Distribution of Membrane Marker Enzymes

	Recovery % $\frac{N+M+L+P+S}{E+N}$	E	N	M	L	P	S	$\frac{P}{E+N}$ = %
5′-Nucleotidase (PM)	93.9 ± 0.42	9.74 ± 0.44	4.82 ± 0.18	2.99 ± 0.11	0.85 ± 0.04	3.66 ± 0.30	1.37 ± 0.09	25.1
Glucose-6-phosphatase (ER)	95.3 ± 0.97	19.85 ± 1.48	3.71 ± 0.24	2.66 ± 0.18	2.03 ± 0.30	13.58 ± 1.84	0.41 ± 0.03	57.6
MAO (OMIM)	96.5 ± 1.48	0.466 ± 0.029	0.136 ± 0.023	0.306 ± 0.008	0.020 ± 0.00	0.083 ± 0.014	0.015 ± 0.002	13.8
Ac-Pase (lysosomes)	95.0 ± 1.03	6.00 ± 0.06	0.82 ± 0.04	1.91 ± 0.14	2.09 ± 0.11	0.89 ± 0.06	0.76 ± 0.03	13.0
Protein	99.0 ± 1.11	196.2 ± 3.54	56.4 ± 2.99	56.6 ± 1.77	9.53 ± 0.84	41.31 ± 2.94	86.21 ± 3.46	16.3

Total activities are expressed as units per gram of liver. Two determinations for each assay were made. Results are given as mean ± standard error of the mean for the four preparations.

Designation of fractions (7, 11): *E* = cytoplasmic extract, *N* = nuclear, *M* = heavy mitochondrial, *L* = light mitochondrial, *P* = microsomal fractions, and *S* = final supernate.

tially the same in both studies.

One simple explanation for the difference could be the choice of different reference parameters: membrane surface area in our study, in contrast to protein in biochemical studies. If ER membranes contained 20% more protein per unit surface area than other membranes, the difference could be explained. The presence of ribosomes on the rough membranes might well add between 10 and 20% protein to that contained in the membrane. There are unfortunately not enough data available that would permit one to either refute or support such a possibility.

It is important to note that the biochemical characteristics of our *P* fractions are comparable to those of Beaufay et al. (5) and Amar-Costesec et al. (1): the protein content and the specific activities of marker enzymes in the *P* fractions were similar; it appears, however, that we recovered a smaller part of both protein and enzymes in the *P* fraction.

Adopting the hypothesis of biochemical homogeneity (11), one could attempt to calculate the relative areas of different membrane classes contributed to the *P* fraction by the following procedure. We know from the study of intact tissue (6, 7) the surface density (S_{Vi}) of each membrane class i in the unit volume of rat liver tissue. Considering the specific weight of liver tissue, we can calculate the membrane surface per unit liver weight (S_{Wi}). Assuming that all of these membranes are still contained in the homogenate derived from 1 g of liver tissue, the surface of i membranes collected in the *P* fraction ($S_{Wi}[P]$) can be estimated by multiplying S_{Wi} by the relative activity of its marker enzyme collected in the *P* fraction ($E_i[P]$):

$$S_{Wi}(P) = S_{Wi} \cdot E_i(P). \tag{7}$$

The relative surface of one membrane class i in the *P* fraction is obtained by

$$S_{Si}(P) = S_{Wi}(P) / \sum_i S_{Wi}(P). \tag{8}$$

This has been done using the biochemical data of Amar-Costesec et al. (1) and our own. We find by this approach that 76 or 78%, respectively, of the membranes in the *P* fraction should be derived from ER.

This calculation rests essentially on the validity of "biochemical homogeneity", i.e., that ER membranes in the various subcellular fractions are similarly "loaded" with the marker enzyme glucose-6-phosphatase. There is some recent evidence that this is not necessarily so;[5] if this should be confirmed, calculations based on Eq. 7 may not be permissible without introducing appropriate weighting factors. But the evidence is too scanty to do this now.

In the present study, the ER membranes in the *P* fractions were also differentiated by staining them cytochemically for glucose-6-phosphatase. By this procedure, 62% of the membrane surface was found to be labeled by the ER marker enzyme. This is evidently in good agreement with the freeze-fracture data but contrasts with the biochemical results. Admittedly, a certain number of labeled vesicles could have been missed if the reaction product had accumulated outside the section thickness; however, a loss of 15% of labeled membranes would be required to bring these data up to 77%, and a loss of this magnitude does not appear likely. A further point is that not all ER membranes of intact hepatocytes become labeled in cytochemical glucose-6-phosphatase reactions. This could explain the low relative ER surface obtained by cytochemistry, but not the freeze-fracture data because these were based on intact tissue standards that encompassed all types of ER membranes.

What Kinds of Errors Could Be Inherent in the Freeze-Fracture Method Used?

(*a*) We must first ask how reliable the tissue standards are. Unfortunately, there are very few investigations on the particle density distributions in freeze-fracture replicas of hepatocyte organelles, and none comparable to ours on intact cells. Packer (28) and Melnick and Packer (23) have analyzed freeze-fracture preparations of inner and outer membranes from isolated rat liver mitochondria. They found that *P* faces of both membranes roughly contain the same particle density, 2,290 and 2,120 Np/μm^2, respectively, which is about two times lower than our density data (4,000–

[5] Combining a stereological analysis of cytochemically labelled fractions with a biochemical analysis, it was found that glucose-6-phosphatase-positive (ER) membranes of *P* fractions may be less densely loaded with glucose-6-phosphatase than those in other fractions. (R. P. Bolender, D. Paumgartner, G. A. Losa, and E. R. Weibel. Unpublished observations.)

4,200). However, our particle density estimates on the EF of the inner (1,230 ± 450 Np/μm^2) and outer membranes (820 ± 420 Np/μm^2) are in reasonable agreement with those of these authors (990 and 558 Np/μm^2).

No data exist on ER membranes. We have found that the particle density distributions given in Fig. 4 were well reproducible, so that we tend to trust this part of the analysis, at least as it relates to our preparation procedures.

(*b*) The question is whether the use made of these standards in unraveling the trimodal distributions found in *P* fractions was appropriate. By restricting the range of ER to $\{\bar{\alpha} \pm 2$ SD$\}$, we have considered only 95% of the potential contribution of ER. Extending this range to $\{\bar{\alpha} \pm 3$ SD$\}$ would exploit 99.95%; but this extended range would be contaminated by contributions of the other membrane types because these ranges would overlap. An evaluation of the distributions given in Fig. 8 reveals that no more than 2–5% of additional ER membranes could be recovered by extending the range.

(*c*) An important source of errors could lie in the possibility that homogenization leads to an artificial shift in particle densities. This is hard to rule out. The fact that the three peaks found in the distributions of Fig. 8 correspond to the modes of the distribution of standards (Fig. 4) suggests that no systematic shift of particle densities has occurred. However, there could have been a statistical shift leading to a greater spread in α in the fractions than in the standards, possibly as a result of temperature-dependent phase transitions (13, 14); this would have resulted in a greater overlap of the distribution profiles. We have therefore attempted an estimate of S_S by considering only a range $\{\alpha \pm 1$ SD$\}$ for each of the three modes of the distributions in Fig. 8; this takes only the central 68% of profiles into consideration and should thus exclude from the sample the regions of possible overlap due to statistical shifts in α. If this is done, we find again 64% of the vesicles in the range characterizing ER. An underestimate of $S_S(er)$ could therefore only be the result of a shift in particle density if this shift was very marked, e.g., from 2,900 to 1,000. But it cannot be excluded that other membranes would then be shifted into the range for ER by a similar mechanism, thus compensating for the loss.

(*d*) The sampling procedure has eliminated a large number of the very small vesicles. How much of the membrane surface has been lost? It is probable that many of the smooth microsomal vesicles of ~40–80-nm diameter were derived from fragmentation of SER tubules. Although these small vesicles make up nearly 12% by number of the vesicle population, it is found that they contribute no more than 2.5% to the membrane surface; but if this is all attributed to ER, then the corrected relative ER surface increases to 66% of all membranes.

It appears from this critique of the method that none of the possible sources of error can explain the low estimate of the relative ER surface in the *P* fractions. In each instance, it was found that the error should be no more than 2–5%. But, evidently, if all these errors were to combine to lead to systematic underestimates of the relative frequency of ER-derived membranes, a cumulative correction for these errors could add as much as 8–10% to the original estimate of $S_S(er)$ which would thus be brought close to the values estimated from biochemical data. Whether such a cumulation of unidirectional errors in the morphometric estimates of relative ER membrane surface is a reasonable assumption remains to be tested; it can neither be ruled out nor supported by currently available evidence.

This communication has exploited a new method for the quantitative differentiation of membrane vesicles as they occur in microsomal fractions, using purely morphological criteria; it could lead to estimates of the relative surface area of ER membranes in these fractions which could be correlated with biochemical data. The values obtained with this method are lower by 12% than what one would generally expect from biochemical information. Which of the data sets are correct? It is not possible yet to say. Although the morphological approach using freeze-fracture preparations could well contain various sources of error, it cannot be excluded that biochemical estimates of the contribution of ER to the *P* fractions are also partly in error because of a possible lack in homogeneity of microsomal membranes with respect to their loading with protein and marker enzymes. Further progress in the attempt to quantitatively correlate membranes as structural components with biochemical entities depends in part on an elucidation of such divergent findings.

This study was supported by grants 3.259.74 and 3.763.76 from the Swiss National Science Foundation. The help of Dr. D. Paumgartner, Dr. M. Baggiolini,

Mr. D. Muellener, Mr. K. Babl, and Miss G. Reber is gratefully acknowledged.

Received for publication 7 September 1977, and in revised form 24 February 1978.

REFERENCES

1. AMAR-COSTESEC, A., H. BEAUFAY, M. WIBO, D. THINÈS-SEMPOUX, E. FEYTMANS, M. ROBBI, and J. BERTHET. 1974. Analytical study of microsomes and isolated subcellular membranes from rat liver. *J. Cell Biol.* **61**:201–212.
2. APPLEMANS, F., R. WATTIAUX, and C. DE DUVE. 1955. Tissue fractionation studies. 5. The association of acid phosphatase with a special class of cytoplasmic granules in rat liver. *Biochem. J.* **59**:438–445.
3. BAUDHUIN, P., H. BEAUFAY, Y. RAHMEN-LI, O. Z. SELLINGER, R. WATTIAUX, P. JACQUES, and C. DE DUVE. 1964. Tissue fractionation studies. 17. Intracellular distribution of monoamine oxidase, aspartate amino transferase, alanine amine transferase, D-amino acid oxidase, and catalase in rat liver tissue. *Biochem. J.* **92**:179–184.
4. BAUDHUIN, P., P. EVRARD, and J. BERTHET. 1967. Electron microscopic examination of subcellular fractions. I. The preparation of representative samples from suspensions of particles. *J. Cell Biol.* **32**:181–191.
5. BEAUFAY, H., A. AMAR-COSTESEC, D. THINÈS-SEMPOUX, M. WIBO, M. ROBBI, and J. BERTHET. 1974. Analytical study of microsomes and isolated subcellular membranes from rat liver. III. Subfractionation of the microsomal fraction by isopycnic and differential centrifugation in density gradients. *J. Cell Biol.* **61**:213–231.
6. BLOUIN, A., R. P. BOLENDER, and E. R. WEIBEL. 1977. Distribution of organelles and membranes between hepatocytes and nonhepatocytes in the rat liver parenchyma. *J. Cell Biol.* **72**:441–455.
7. BOLENDER, R. P., D. PAUMGARTNER, G. LOSA, D. MUELLENER, and E. R. WEIBEL. 1978. Integrated stereological and biochemical studies on hepatocytic membranes. I. Membrane recoveries in subcellular fractions. *J. Cell Biol.* **77**:565–583.
8. BRANTON, D. 1971. Freeze-etching studies of membrane structure. *Philos. Trans. R. Soc. Lond. B Biol. Sci.* **261**:133.
9. BRANTON, D., N. B. GILULA, M. J. KARNOVSKY, M. MOOR, K. MÜHLETHALER, D. H. NORTHCOTE, L. PACKER, B. SATIR, P. SATIR, V. SPETH, L. A. STAEHLIN, R. L. STEERE, and R. S. WEINSTEIN. 1975. Freeze-etching nomenclature. *Science (Wash., D.C.)* **190**:54–56.
10. CHALCROFT, J. P., and S. BULLIVANT. 1970. An interpretation of liver cell membrane and junction structure based on observations of freeze-fracture replicas of both sides of the fracture. *J. Cell Biol.* **47**:49–60.
11. DE DUVE, C., B. C. PRESSMAN, R. GIANETTO, R. WATTIAUX, and F. APPLEMANS. 1955. Tissue fractionation studies. 6. Intracellular distribution patterns of enzymes in rat liver tissue. *Biochem. J.* **60**:604–617.
12. DEMSEY, A. E., and E. R. KENNEDY. 1972. A freeze-etch study of the cell wall and cytoplasmic membrane of *Staphylococcus aureus*. *J. Microsc. (Paris)*. **13**:343–348.
13. DUPPEL, W., and G. DAHL. 1976. Effect of phase transition on the distribution of membrane-associated particles in microsomes. *Biochim. Biophys. Acta.* **426**:408–417.
14. DUPPEL, W., and V. ULLRICH. 1976. Membrane effects on drug monooxygenation activity in hepatic microsomes. *Biochim. Biophys. Acta.* **426**:399–407.
15. EMMELOT, P. C., J. BOS, E. L. BENEDETTI, and P. H. RÜNKE. 1964. Studies on plasma membranes. I. Chemical composition and enzyme content of plasma membranes isolated from rat liver. *Biochim. Biophys. Acta.* **90**:126–145.
16. GOODENOUGH, D. A., and J. P. REVEL. 1970. A fine structural analysis of the intercellular junctions in the mouse liver. *J. Cell Biol.* **45**:272–290.
17. HACKENBROCK, C. 1972. States of activity and structure in mitochondrial membranes. *Ann. N.Y. Acad. Sci.* **195**:492–505.
18. KRAEHENBÜHL, J. P., and J. D. JAMIESON. 1976. Enzyme labeled antibody markers for electron microscopy. *In* Methods in Immunology and Immunocytochemistry. C. A. Williams, and M. W. Chase, editors. Academic Press, Inc., New York. 482–495.
19. KREIBICH, G., A. L. HUBBARD, and D. D. SABATINI. 1974. On the spatial arrangement of proteins in microsomal membranes from rat liver. *J. Cell Biol.* **60**:616–627.
20. LESKES, A., P. SIEKEVITZ, and G. E. PALADE. 1971. Differentiation of endoplasmic reticulum in hepatocytes. II. Glucose-6-phosphatase in rough microsomes. *J. Cell Biol.* **49**:288–302.
21. LOSA, G. 1976. Rat liver plasma membrane vesicles obtained by homogenization retain outside-out orientation. 10th International Congress of Biochemistry. Hamburg 05-4-280. Brünners Edit., Breidenstein K. G., Frankfurt, Germany. 282.
22. LOWRY, O. H., N. J. ROSEBROUGH, A. L. FARR, and R. J. RANDALL. 1951. Protein measurement with the folin phenol reagent. *Biochem. J.* **193**:265–275.
23. MELNICK, R. L., L. PACKER. 1971. Freeze-fracture faces of inner and outer membranes of mitochondria. *Biochim. Biophys. Acta.* **253**:503–508.
24. MOOR, H. 1969. Freeze-etching. *Int. Rev. Cytol.* **25**:391–412.

25. MOOR, H., and K. MÜHLETHALER. 1963. Fine structure in freeze-etched yeast cells. *J. Cell Biol.* **17**:609–628.
26. MÜHLETHALER, K. 1971. Studies on freeze-etching of cell membranes. *Int. Rev. Cytol.* **31**:1–19.
27. ORCI, L., A. MATTER, and C. ROUILLER. 1971. A comparative study of freeze-etched replicas and thin sections of rat liver. *J. Ultrast. Res.* **35**:1–19.
28. PACKER, L., 1972. Functional organization of intramembrane particles of mitochondrial inner membranes. *J. Bioenerg.* **3**:115–127.
29. REDDY, J. K., J. P. TEWARI, D. J. SVOBODA, and S. K. MALHOTRA. 1974. Identification of the hepatic microbody membrane in freeze-fracture replicas. *Lab. Invest.* **31**:268–275.
30. TILLACK, T. W., R. E. SCOTT, and V. T. MARCHESI. 1970. Studies on the chemistry and function of the intramembranous particles observed by freeze-etching of red cell membranes. *J. Cell Biol.* **47**:213a. (Abstr.)
31. WEIBEL, E. R., and R. P. BOLENDER. 1973. Stereological techniques for electron microscopic morphometry. *In* Principles and Techniques of Electron Microscopy. M. A. Hayat, editor. Van Nostrand Reinhold Company, New York, **3**:237–296.
32. WEIBEL, E. R., G. LOSA, and R. P. BOLENDER. 1976. Stereological method for estimating relative membrane surface area in freeze-fracture preparations. *J. Microsc. (Oxf.)*. **107**:255–266.
33. WEIBEL, E. R., and D. PAUMGARTNER. 1978. Integrated stereological and biochemical studies on hepatocytic membranes. II. Correction of section thickness effect on volume and surface density estimates. *J. Cell Biol.* **77**:584–597.